Finally, the following inequality holds:

$$\sum_{s=k_0}^{k-1} a^{k-1-s} e^T(s)e(s) \le \lambda^2 \sum_{s=k_0}^{k-1} (ca)^{k-1-s} w^T(s)w(s). \quad (48)$$

Accumulating both sides of (45) from $k = 1$ to $k = +\infty$ and changing the order of summation yields

$$\sum_{s=k_0}^{+\infty} e^T(s)e(s) \le \frac{1-a}{1-ca}\lambda^2 \sum_{s=k_0}^{+\infty} w^T(s)w(s). \quad (49)$$

By similar analysis for $k \in [k_l + t_l, k_{l+1})$, the above inequality also holds. Thus, the l_2 gain from the noise signal to the estimation error is obtained as $\gamma = \sqrt{((1-a)/(1-ca))}\,\lambda$. This completes the proof.

REFERENCES

[1] S. Haykin, *Neural Networks: A Comprehensive Foundation*. Englewood Cliffs, NJ: Prentice-Hall, 1998.

[2] J. Cao and J. Liang, "Boundedness and stability for Cohen-Grossberg neural network with time-varying delays," *J. Math. Anal. Appl.*, vol. 296, no. 2, pp. 665–685, 2004.

[3] Z. Wang, Y. Liu, and X. Liu, "On global asymptotic stability of neural networks with discrete and distributed delays," *Phys. Lett. A*, vol. 345, nos. 4–6, pp. 299–308, 2005.

[4] H. Huang, D. W. C. Ho, and J. Cao, "Analysis of global exponential stability and periodic solutions of neural networks with time-varying delays," *Neural Netw.*, vol. 18, no. 2, pp. 161–170, 2005.

[5] Y. He, G. Liu, D. Rees, and M. Wu, "Stability analysis for neural networks with time-varying interval delay," *IEEE Trans. Neural Netw.*, vol. 18, no. 6, pp. 1850–1854, Nov. 2007.

[6] Y. Liu, Z. Wang, and X. Liu, "Robust stability of discrete-time stochastic neural networks with time-varying delays," *Neurocomputing*, vol. 71, nos. 4–6, pp. 823–833, 2008.

[7] C. Song, H. Gao, and W. Zheng, "A new approach to stability analysis of discrete-time recurrent neural networks with time-varying delay," *Neurocomputing*, vol. 72, nos. 10–12, pp. 2563–2568, 2009.

[8] Z. Wu, H. Su, J. Chu, and W. Zhou, "Improved delay-dependent stability condition of discrete recurrent neural networks with time-varying delays," *IEEE Trans. Neural Netw.*, vol. 21, no. 4, pp. 692–697, Apr. 2010.

[9] H. Huang, Y. Qu, and H. Li, "Robust stability analysis of switched Hopfield neural networks with time-varying delay under uncertainty," *Phys. Lett. A,* vol. 345, nos. 4–6, pp. 345–354, 2005.

[10] K. Yuan, J. Cao, and H. Li, "Robust stability of switched Cohen–Grossberg neural networks with mixed time-varying delays," *IEEE Trans. Syst., Man, Cybern. B, Cybern.*, vol. 36, no. 6, pp. 1356–1363, Dec. 2006.

[11] H. Zhang, Z. Liu, and G. Huang, "Novel delay-dependent robust stability analysis for switched neutral-type neural networks with time-varying delay via SC technique," *IEEE Trans. Neural Netw.*, vol. 40, no. 6, pp. 1480–1491, Dec. 2010.

[12] L. Wu, Z. Feng, and W. Zheng, "Exponential stability analysis for delayed neural networks with switching parameters: Average dwell time approach," *IEEE Trans. Neural Netw.*, vol. 21, no. 10, pp. 1396–1407, Sep. 2010.

[13] Z. Wu, P. Shi, H. Su, and J. Chu, "Delay-dependent stability analysis for switched neural networks with time-varying delay," *IEEE Trans. Syst., Man, Cybern. B, Cybern.*, vol. 41, no. 6, pp. 1522–1530, Dec. 2011.

[14] D. Zhang and L. Yu, "Passivity analysis for discrete-time switched neural networks with various activation functions and mixed time delays," *Nonlinear Dyn.*, vol. 67, no. 1, pp. 403–411, 2012.

[15] Z. Wang, D. W. C. Ho, and X. Liu, "State estimation for delayed neural networks," *IEEE Trans. Neural Netw.*, vol. 16, no. 1, pp. 279–284, Jan. 2005.

[16] Y. He, Q. G. Wang, M. Wu, and C. Lin, "Delay-dependent state estimation for delayed neural networks," *IEEE Trans. Neural Netw.*, vol. 17, no. 4, pp. 1077–1081, Jul. 2006.

[17] Y. Liu, Z. Wang, and X. Liu, "Design of exponential state estimators for neural networks with mixed time delays," *Phys. Lett. A*, vol. 364, nos. 5–7, pp. 401–412, 2007.

[18] S. Mou, H. Gao, W. Qiang, and Z. Fei, "State estimation for discrete-time neural networks with time-varying delays," *Neurocomputing*, vol. 72, nos. 1–3, pp. 643–647, 2008.

[19] H. Huang and G. Feng, "Delay-dependent H_∞ and generalized H_2 filtering for delayed neural networks," *IEEE Trans. Circuits Syst. I*, vol. 56, no. 4, pp. 846–857, Apr. 2009.

[20] C. K. Ahn and M. Song, "L_2–L_∞ filtering for time-delayed switched hopfield neural networks," *Int. J. Innov. Comput. I*, vol. 7, no. 4, pp. 1831–1844, 2011.

[21] L. Zhang and H. Gao, "Asynchronously switched control of switched linear systems with average dwell time," *Automatica*, vol. 46, no. 5, pp. 953–958, 2010.

[22] L. Zhang, N. Cui, M. Liu, and Y. Zhao, "Asynchronous filtering of discrete-time switched linear systems with average dwell time," *IEEE Trans. Circuits Syst. I*, vol. 58, no. 5, pp. 1109–1118, May 2011.

[23] Z. Xiang, C. Liang, and Q. Chen, "Robust L_2–L_∞ filtering for switched systems under asynchronous switching," *Commun. Nonlin. Sci.* vol. 16, no. 8, pp. 3303–3318, 2011.

[24] D. Zhang, L. Yu, and W. Zhang, "Delay-dependent fault detection for switched linear systems with time-varying delays-the average dwell time approach," *Signal Process.*, vol. 91, no. 4, pp. 832–840, 2011.

[25] X. Jiang, Q. Han, and X. Yu, "Stability criteria for linear discrete-time systems with interval-like time-varying delay," in *Proc. Amer. Control Conf.*, vol. 2. Portland, OR, Jun. 2005, pp. 2817–2822.

[26] M. Dehghan and C. Ong, "Discrete-time switched linear system with constraints: Characterization and computation of invariant sets under dwell time consideration," *Automatica*, to be published.

[27] S. Boyd, L. E. Ghaoui, E. Feron, and V. Balakrishinan, "SIAM studies in applied mathematics," in *Proc. Lin. Matrix Inequal. Syst. Control Theory*, Philadelphia, PA, 1994, pp. 1–205.

Weighted Least-Squares Approach for Identification of a Reduced-Order Adaptive Neuronal Model

Lingfei Zhi, Jun Chen, Peter Molnar, and Aman Behal

***Abstract*— This brief is focused on the parameter estimation problem of a second-order adaptive quadratic neuronal model. First, it is shown that the model discontinuities at the spiking instants can be recast as an impulse train driving the system dynamics. Through manipulation of the system dynamics, the membrane voltage can be obtained as a *realizable* model that is linear in the unknown parameters. This linearly parameterized realizable model is then utilized inside a prediction error-based framework to design a dynamic estimator that allows for rapid estimation of model parameters under a persistently exciting input current injection. Simulation results show the feasibility of this approach to predict multiple neuronal firing patterns.**

Manuscript received October 19, 2010; revised February 1, 2012; accepted February 5, 2012. Date of publication February 27, 2012; date of current version May 2, 2012. The work was supported by Award R15NS062402 from NINDS.

L. Zhi is with the Department of Electrical Engineering and Computer Science, University of Central Florida, Orlando, FL 32826 USA (e-mail: zlfziegfeld@gmail.com).

J. Chen is with Iowa State University, Ames, IA 50010 USA (e-mail: junchen@mail.ucf.edu).

P. Molnar is with the Department of Zoology, University of West Hungary, Sopron 9400, Hungary (e-mail: pmolnar@pminfonet.com).

A. Behal is with the Department of Electrical Engineering and Computer Science and the NanoScience Technology Center, University of Central Florida, Orlando, FL 32826 USA (e-mail: abehal@mail.ucf.edu).

Color versions of one or more of the figures in this paper are available online at http://ieeexplore.ieee.org.

Digital Object Identifier 10.1109/TNNLS.2012.2187539

Results using both synthetic data (obtained from a detailed ion-channel-based model) and experimental data (obtained from *in vitro* embryonic rat motoneurons) suggest directions for further work.

***Index Terms*— Adaptive spiking behavior, characterization, parameter estimation, quadratic integrate-and-fire, spiking neuron.**

I. Introduction

In the past decade, the spiking neuron model has been extensively researched for computational efficiency. Although, Hodgkin–Huxley models [1] with tens of ion channels can accurately reproduce most types of neuronal behavior, it is difficult to tune hundreds of parameters associated with such models. Over the last few years, the efficiency and versatility of spiking neural networks has been extensively demonstrated in literature, e.g., [2]– [10]. However, it is computationally prohibitive to simulate large networks based on complex underlying neuronal models-this limitation effectively restricts neuronal network simulations to only a handful of neurons at a time [11]. Although a simple integrate-and-fire model [12] is computationally tractable, it can only produce a few types of firing patterns [13]. In [11], a recovery variable is introduced to the simple spiking model-this variable is intended to capture adaptation by accounting for the activation of K^+ ionic currents and inactivation of Na^+ ionic currents. Such an adaptive quadratic spiking model has the ability to qualitatively reproduce major types of firing patterns and is computationally tractable for large network simulation [13], [14]. Although the adaptive quadratic spiking model has been discussed at great length in [11], [13], and [14], a systematic technique to tune the parameters of such a model to experimental data is, however, still needed. The importance of characterizing the underlying neuronal behavior is of critical importance to subsequent estimation of the weights of a neural network that has one or more types of spiking neurons as its building blocks. Specifically, [15] states that the identification problem in a black-box formulation such as a neural network is more likely to be efficient and successful if the network parameters (i.e., weights) are estimated post discovery of the underlying neuronal behavior parameters.

Generally, there are two approaches to match the proposed model to experimental data - manual and automatic [16]. In the manual approach, one can manually change the model parameters to produce the desired biological behavior, e.g., in [17], by hand-tuning each parameter individually, an adaptive exponential integrate-and-fire neuron model is tuned to fit a detailed Hodgkin–Huxley-based model. Although a manual approach may yield good results, it is labor–intensive and depends mainly on the researcher's experience. Furthermore, it is unrealistic to suppose that one could process all data comparisons manually [18], thus, automatic parameter estimation methods are necessary. In [19], a database of single-compartment model neurons is constructed by exploring the entire parameter space - this approach is only practical when the parameter space has a low dimension. In [20], several automatic parameter searching techniques, including conjugate gradient, genetic algorithm, simulated annealing, and stochastic search, are reviewed and compared in fitting a multidimensional model to experimental data. However, these methods are computationally expensive since they require a large number of evaluations of the model.

Motivated by the versatility and computational efficiency of the adaptive quadratic model given in [11], we propose a weighted least square based estimation method to automatically estimate the parameters of the aforementioned model. By casting the discontinuities in the state variables at the spiking instants as an impulse train driving the system dynamics, the model can be manipulated such that the neuronal output is representable as a model which is linear in the unknown parameters. Furthermore, the model is realizable in that it only depends on filtered versions of the input current and the output voltage at the cell membrane. Based on this novel formulation of the model, a weighted least squares-based estimation approach is able to asymptotically drive the parameter estimation errors to zero even in the presence of measurement noise.

The remainder of this brief is organized as follows. In Section II, we present the adaptive quadratic model and the problem statement. Technical details for model manipulation and the identification mechanism are provided in Section III. Section IV provides detailed procedure for carrying out the identification followed by simulation results and discussions. Appropriate conclusions are drawn in Section V.

II. Model

A simple adaptive quadratic spiking model can be described by the nonlinear state equations [11]

$$\frac{dv}{dt} = k_1 v^2 + k_2 v + k_3 - k_4 (u - i) \tag{1}$$

$$\frac{du}{dt} = a(bv - u) \tag{2}$$

with the post-spike resetting

$$if\ v = V_p, \qquad \text{then} \begin{cases} v \to c \\ u \to u + d. \end{cases} \tag{3}$$

Here, v denotes the membrane potential and is the output of the system while u is the immeasurable membrane recovery state variable. The injected current and/or synaptic current affect the system dynamics via the input variable i. At the membrane potential peak V_p, the state variables are reset according to (3) where c denotes the post-spike reset value of the membrane potential while d denotes the amount of spike adaptation of the recovery variable. The parameters k_4 and a denote the time scale of the two state variables, b is the level of subthreshold adaptation, while k_1, k_2, and k_3 are linked to the spike initiation behavior of the neuron. The vector of unknown parameters is defined as $\theta_o = (k_1, k_2, k_3, k_4, a, b, c, d) \in \Re^8$. Our goal is to estimate θ_o such that the spiking pattern of the quadratic spiking model of (1)–(3) with the estimated parameters can replicate the spiking behavior observed in the simulated/experimentally obtained data.

III. Estimation Technique

A. Discontinuities at Spike Times

Motivated by the desire to utilize a prediction error based automatic estimation method, we first integrate the reset

discontinuities given by (3) into the state equations of (1) and (2)-this is done with the purpose of manipulating the system dynamics into a form that is amenable to linear parameterized (LP) model development. Since the resetting of the membrane potential in (3) always happens at the time when v equals to the peak value V_p, it can be considered as a jump of size $c - V_p$, which can be modeled as a step input as follows:

$$v \to v + (c - V_p)s(t - t_{s_j}) \tag{4}$$

where $s(t - t_{s_j})$ denotes a unit step at the occurrence of the jth spike at time t_{s_j}. By taking the time derivative of (4), and combining with (1), one obtains

$$\frac{dv}{dt} = k_1 v^2 + k_2 v + k_3 - k_4 (u - i) + (c - V_p)\delta(t - t_{s_j}) \tag{5}$$

where $\delta(t - t_{s_j})$ denotes a unit impulse at time t_{s_j}. Note that (5) correctly represents the v dynamics $\forall\ t_{s_{j-1}} < t < t_{s_{j+1}}$. It is easy to see that the v dynamics valid over all spiking instants can be obtained by introducing a train of impulses into the dynamics as follows:

$$\frac{dv}{dt} = k_1 v^2 + k_2 v + k_3 - k_4 (u - i) + (c - V_p) \sum_j \delta(t - t_{s_j}). \tag{6}$$

Similarly, the discontinuity in u at a spike instant t_{s_j} can also be modeled as a step input of size d as follows:

$$u \to u + ds(t - t_{s_j}). \tag{7}$$

Following arguments similar to those made above, and utilizing (2) and (7), the u dynamics valid over all spiking instants can be compactly described as

$$\frac{du}{dt} = -au + abv + d \sum_j \delta(t - t_{s_j}). \tag{8}$$

Thus, the dynamics of (1)–(3) have been compactly recast into the dynamics of (6) and (8).

B. Linear Parameterization

The nonlinear dynamics of (6) and (8) can be further developed to obtain a linear-in-parameters model that depends only on measurable variables. By substituting the Laplace transformation of (8) into that of (6), and applying a low pass filter of the form

$$\frac{1}{A} = \frac{1}{s^2 + \beta_1 s + \beta_0} \tag{9}$$

to avoid the model dependency on the derivatives of the input and the output [21], one can obtain the following expression after rearranging terms conveniently:

$$\begin{aligned} V = {} & \frac{k_1(s + a)L(V^2)}{A} + \frac{k_4(s + a)I}{A} + \frac{k_3 a}{sA} \\ & + \frac{[(k_2 + \beta_1 - a)s + k_2 a + \beta_0 - k_4 ab]V}{A} \\ & + \frac{\left[(c - V_p)(s + a) - k_4 d\right] \sum_j \exp(-s t_{s_j})}{A} \\ & + \frac{(s + a)v(0)}{A} + \frac{k_3}{A} - \frac{k_4 u(0)}{A} \end{aligned} \tag{10}$$

where $L(\cdot)$ denotes the Laplace operator, s denotes the Laplace variable, while V and I represent the Laplace transform of v and i, respectively. To reduce parameter dimensionality, the signals presented in the last row of (10) can be excluded from further analysis since they do not persist beyond an initial transient. By a slight abuse of notation, a compact representation for a LP *realizable* model is obtained as follows:

$$v = W\left(v, i, t_{s_j}\right)\theta \tag{11}$$

where $W\left(v, i, t_{s_j}\right) \in \Re^{1\times 9}$ is a realizable regression vector which is defined as follows:

$$\begin{aligned} W = \Bigg[& \frac{s}{A}L(v^2), \frac{1}{A}L(v^2), \frac{s}{A}V, \frac{1}{A}V, \frac{1}{sA}, \frac{s}{A}I, \frac{1}{A}I, \\ & \frac{s}{A}\sum_j \exp(-s t_{s_j}), \frac{1}{A}\sum_j \exp\left(-s t_{s_j}\right) \Bigg] \end{aligned} \tag{12}$$

while $\theta \in \Re^9$ is an unknown parameter vector which is defined as follows:

$$\begin{aligned} \theta = [& k_1,\ k_1 a, k_2 + \beta_1 - a, k_2 a + \beta_0 - k_4 ab, \\ & k_3 a, k_4, k_4 a, c - V_p, a(c - V_p) - k_4 d]^T. \end{aligned} \tag{13}$$

Note that the derived parameter vector θ is an overparameterized by (1) function of the original parameter set θ_o.

C. Weighted Least Squares Algorithm

Based on the LP model derived above in (11), a prediction error-based estimation algorithm can be developed. Since measurement noise is inevitable when dealing with biological systems, robustness to presence of noise is a primary consideration when choosing an estimation algorithm. Therefore, algorithms that are not robust under noise, e.g., adaptation laws based on the gradient of the instantaneous prediction error, are not considered for implementation. Since least squares estimation is known to be robust to noise [21], it is pursued here. We begin by defining a prediction error as follows:

$$e = \hat{v} - v = W(\cdot)\hat{\theta} - v \tag{14}$$

where $\hat{\theta} \in \Re^9$ denotes the parameter estimate vector while $\hat{v} = W(\cdot)\hat{\theta}$ denotes the predicted output. The standard objective function for least squares estimation is given as follows:

$$J = \int_0^t e^2(r)dr = \int_0^t \left\| v(r) - W(r)\hat{\theta}(t) \right\|^2 dr. \tag{15}$$

It is important to consider the fact that the behavior of the neuron around the time of spike initiation is much more important than its behavior at all other times since our objective is to predict neuronal spiking patterns. However, since the contribution of the spike in the function J is rather small due to its short interval of occurrence compared with the time of occurrence of pre- and post-spiking activity, the objective function needs to be weighted. Thus, we redefine the objective function as follows:

$$J = \int_0^t k(r)e^2(r)dr = \int_0^t k(r) \left\| v(r) - W(r)\hat{\theta}(t) \right\|^2 dr \tag{16}$$

where $k(t)$ denotes a weight term which can be chosen appropriately near the time of spike occurrence. When the

objective function is minimized (by setting its derivative with respect to the parameter estimate vector to zero), we obtain

$$\int_0^t k(r)W^T(r)W(r)dr\hat{\theta}(t) = \int_0^t k(r)W^T(r)v(r)dr.$$

By defining

$$P = \left[\int_0^t k(r)W^T(r)W(r)dr\right]^{-1} \tag{17}$$

one can easily obtain the dynamics for parameter estimation as follows:

$$\dot{\hat{\theta}} = -k(t)P(t)W^T(t)e \tag{18}$$

$$\dot{P} = -k(t)PW^T(t)W(t)P. \tag{19}$$

By defining $\tilde{\theta} = \hat{\theta} - \theta \in \Re^9$ as the parameter estimation error and utilizing (17) and (18), the time derivative of a Lyapunov function $V_1(t) \triangleq \tilde{\theta}^T P^{-1}\tilde{\theta}$ can be found to be $\dot{V}_1(t) = -\tilde{\theta}^T W^T W\tilde{\theta}$, which implies by uniform continuity arguments and Barbalat's Lemma [21] that

$$\lim_{t\to\infty} W\tilde{\theta} = 0. \tag{20}$$

If the regressor matrix W is persistently exciting, it implies that there must exist positive constants α_1 and T such that [21]

$$\int_t^{t+T} W^T W dr \geq \alpha_1 I_9 \qquad \forall t \geq 0. \tag{21}$$

By premultiplying (20) with $W^T(\cdot)$ and integrating the equation for T time units, one obtains

$$\lim_{t\to\infty} \int_t^{t+T} W^T W\tilde{\theta} dr = 0 \tag{22}$$

which implies from (21) that the only solution of (22) is $\lim_{t\to\infty} \tilde{\theta}(t) = 0$.

Remark 1: If parametric drift is observed during estimation, a robust modification such as σ-modification or projection modification can be applied to the proposed algorithm.

IV. Procedure And Results

A. Estimation Procedure

We have tuned the model to match four types of reference data: 1) membrane voltage data from the adaptive quadratic model itself-this is used to test the validity of our approach; 2) noisy version of membrane voltage data from the adaptive quadratic model-this is to test the robustness of the proposed method; 3) membrane voltage data from a detailed ion-channel-based (Hodgkin–Huxley type) model; and 4) *in vitro* experimental data collected in our laboratory from embryonic rat motoneurons.

The injected current input i needs to be properly designed to ensure the persistent excitation of the regression matrix $W(\cdot)$ of (12), which is a prerequisite for the estimated parameters to converge to their true values. Since a reference containing a single sinusoidal frequency can estimate two parameters for linear system dynamics [21], and the square nonlinearity in the output generates extra excitation as well, a combination of sinusoids at four different frequencies is utilized to estimate the parameter vector of (13). Specifically, the waveform type employed for generating the input i is given as follows:

$$i = I_1\sin(\omega_1 t) + I_2\sin(\omega_2 t) + I_3\sin(\omega_3 t) + I_4\sin(\omega_4 t) \tag{23}$$

where I_i and $\omega_i \ \forall\ i = 1, 2, 3, 4$ denote the amplitudes and frequencies of the underlying sinusoids, respectively.

Given the reference data generated through (23) and the recorded output v, the data is processed to determine V_p and the spike instants t_{s_j}. To obtain the regression signals (12), the parameters for the low-pass filter of (9) are designed so that the cut-off frequency of the low-pass filter is upperbounded by the measurement noise in the system and lowerbounded by the highest frequency of the input current. The estimation algorithm is implemented according to (14), (18), and (19).[1] The identification algorithm is switched on at $t = 20$ ms in order to allow for the transient effects to pass as discussed below (10). After estimation, the original parameters $\theta_o = (k_1, k_2, k_3, k_4, a, b, c, d)$ need to be retrieved from the estimated-derived parameter vector $\hat{\theta}$. According to (13), the relationship between the original parameter and derived parameter θ can be represented as a nonlinear function $\theta = \theta(\theta_o)$. A nonlinear equation solver or an optimization algorithm (e.g., nonlinear optimization toolbox in MATLAB) can be utilized to select the best value for θ_o that minimizes the difference between $\theta(\theta_o)$ and estimated $\hat{\theta}$. Finally, to evaluate the validity of the estimated model parameters, either step or periodic input currents are utilized to compare membrane voltage data from actual and estimated system models.

B. Results from Quadratic Reference Data

In this section, we identify the model parameters based on reference data generated by the quadratic model itself-here, the membrane voltage measurements are assumed to be noiseless. For the reference data generation, the parameters for the injected current (23) are chosen as follows:

$$I_1 = 3.9 \quad I_2 = 13 \quad I_3 = 9.1 \quad I_4 = 15.6$$
$$\omega_1 = 0.5 \quad \omega_2 = 2.25 \quad \omega_3 = 2.0 \quad \omega_4 = 2.5$$

where the units of currents and frequencies are nA and rad·ms^{-1}, respectively. Given this reference input signal, various sets of model parameters are utilized to generate corresponding membrane potential waveforms in order to demonstrate the versatility of the approach. We first present identification results from a rapidly adapting receptor (i.e., receptor initially fires and then quickly stops firing in response to steady input), data for which are generated by using model parameters as follows:

$$\theta_o = (0.04, 5, 140, 1, 0.02, 0.2, -65, -0.5).$$

Fig. 1(a) shows the output of the exact model to the injected reference sinusoidal input current with the parameters described above, as well as the predicted behavior in the estimation process. The rapid convergence of parameters is

[1] As stated in [21], from an information theoretic perspective, P denotes the estimation covariance matrix, thus, $P(0)$ should be chosen to represent the covariance of the initial parameter estimates. In the absence of this knowledge, $P(0)$ was chosen to be diagonal for simplicity.

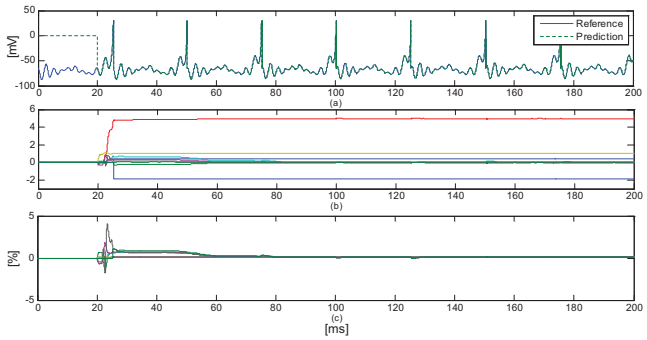

Fig. 1. (a) Spike trains of target data and prediction of a rapidly adapting receptor during identification process. (b) Rapid convergence of estimated parameters. (c) % estimation error of parameters.

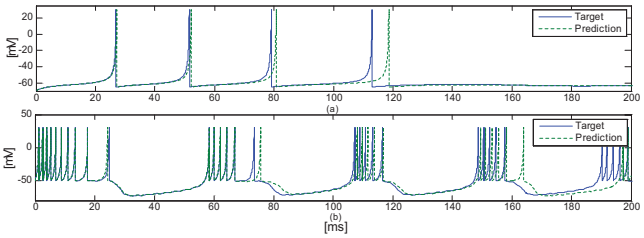

Fig. 2. Validation results. (a) Spike trains of target and prediction data for the rapidly adapting receptor under step input. (b) Spike trains of target and prediction data for a tonic bursting neuron under step input.

shown in Fig. 1(b) while relative parameter estimation errors, defined as $\left(\hat{\theta}/\theta - 1\right) \times 100\%$, are shown in Fig. 1(c). The convergence of the prediction error is clearly implied from the significant similarity in the two spiking trains in Fig. 1(a). For validation of our identified model, a step current $i = 3.5$ nA was applied to the exact and the estimated quadratic models. Fig. 2(a) shows that the prediction emulates the rapid adaptation behavior of the exact model as expected, in fact, the prediction correctly estimates the firing pattern and the firing rate.

We next considered another important firing pattern, namely, tonic bursting, which can be found in the chattering neurons in the cat neocortex [22]. To generate the reference data for identification, the model parameters were chosen as follows:

$$\theta_o = (0.04, 5, 140, 1, 0.02, 0.2, -50, 2).$$

To evaluate the efficacy of the identification, a 15-nA step input current was applied to both models. The prediction in Fig. 2(b) is shown to have a small delay as compared with the reference, however, the prediction successfully follows the pattern of target data. Furthermore, the information encoded in the interspike frequency is conserved, both the target and prediction show ∼20 bursts/s while the firing frequency within a burst is ∼2.5 spikes/ms.

C. Results from Noisy Quadratic Reference Data

To simulate noise in a biological system, the reference membrane potential data obtained from the exact quadratic model was corrupted by adding white noise with an SNR of 40 dB. The result for a neuron which fires with decreasing frequency is shown in Fig. 3. The model parameters were

$$\theta_o = (0.04, 5, 140, 1, 0.02, 0.2, -65, 2).$$

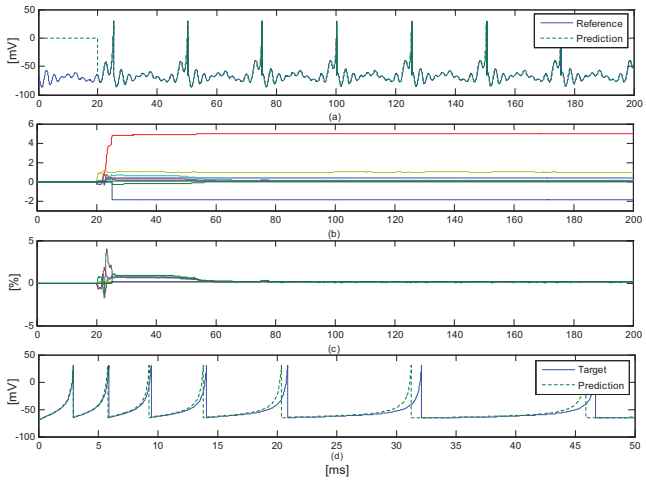

Fig. 3. (a) Spike trains of target data and prediction of a rapidly adapting receptor under noise during the estimation process. (b) Rapid convergence of estimated parameters. (c) % estimation error of parameters. (d) Spike trains of target and prediction data under step input.

The sinusoidal input fed for identification is the same as described above. A step input of $i = 12.5$ nA was injected for validation. Fig. 3 shows that the proposed approach is robust to noise although there is a slight amount of under-adaptation in the prediction curve under step input. However, the firing pattern and rate are successfully predicted with accuracy.

D. Results from Hodgkin–Huxley Model Data

In this section, the goal was to estimate quadratic model parameters that would replicate spiking patterns from a detailed ion-channel-based (Hodgkin–Huxley type) model [23] with parameters from [24]. The injected current parameters for generating reference data were chosen as

$$I_1 = 2.1 \quad I_2 = 7.0 \quad I_3 = 4.9 \quad I_4 = 8.4$$
$$\omega_1 = 0.5 \quad \omega_2 = 2.0 \quad \omega_3 = 2.25 \quad \omega_4 = 2.5$$

where the units of current and frequency are as before. The weight term k defined in (16) was chosen to be time-varying during the spiking intervals (weighted 2 initially and then decaying proportional to the square of the spike number) while it was chosen to be 1 everywhere else. Under sinusoidal input injection given by (23), the rapid convergence of parameters in the estimation process and the match between adaptive quadratic model and detailed regular spiking model are shown in Fig. 4. Evidently, the firing rate and pattern between the target and the prediction are remarkably close. While the prediction results are acceptable when the input waveform used for validation is of similar type as in the identification, we were not able to replicate the experimental behavior under a step input. We discuss this issue at length in Section IV-F.

E. Results from Experimental Data

In this section, we show the ability of the estimated model to replicate *in vitro* experimental data using embryonic rat motoneurons. Primary cultures of embryonic rat motoneurons were prepared according to NIH guidelines and in agreement with the Institutional Animal Care and Use Committee

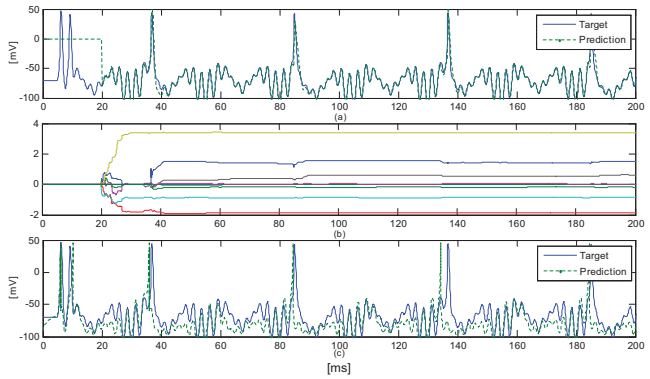

Fig. 4. (a) Spike trains of target data from a detailed ion-channel based model and prediction in the estimation process. (b) Rapid convergence of estimated parameters. (c) Spike trains of target data and prediction during validation process.

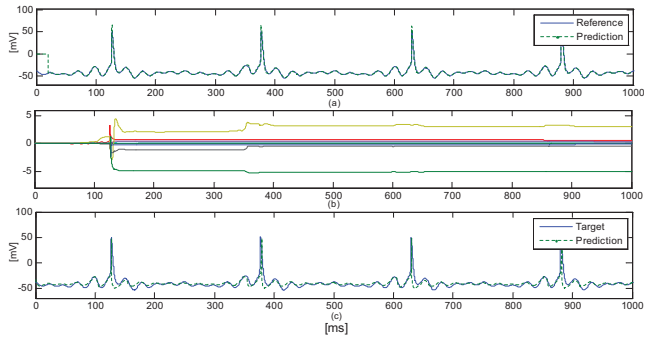

Fig. 5. (a) Spike trains of target data from *in vitro* embryonic motoneuron and prediction in the estimation process. (b) Rapid convergence of estimated parameters. (c) Spike trains of target data and prediction during validation process.

approved protocol. Voltage recordings were acquired by performing conventional whole-cell patch clamp on the cultured cells between days 7 and 14 in culture. The extracellular solution was Neurobasal culture medium, with pH adjusted to 7.3. Patch pipets were filled with intracellular solution. Signals were filtered at 3 kHz and digitized at 10 kHz with an Axon Digidata 1322A interface. Data recording and initial analysis were performed with pClamp 10 software (Axon). The injected current parameters for generating the sinusoidal reference data were chosen as

$$I_1 = 0.075 \quad I_2 = 0.25 \quad I_3 = 0.175 \quad I_4 = 0.3$$
$$\omega_1 = 0.05 \quad \omega_2 = 0.225 \quad \omega_3 = 0.2 \quad \omega_4 = 0.25$$

where the units of current and frequency are as before. The weight term k was chosen in the same manner as described above in Section IV-D. Fig. 5(a) shows the reference data and the prediction during the model identification phase. Fig. 5(b) shows rapid convergence of parameter estimates. From Fig. 5(c), it is clear to see the match between the target and prediction data during model validation. The target firing rate and pattern are successfully reproduced. As was the case in Section IV-D, we were unable to replicate the behavior of the motoneuron under step input.

F. Discussion

The results for prediction of reference data generated from the quadratic model itself show good prediction and robustness under noise, which demonstrate the efficacy of the estimation algorithm and approach. However, the prediction of the detailed ion-channel model and experimental data merits more discussion. Specifically, there are differences between the data obtained from the detailed model and the assumptions made by the quadratic model of [11]. For example, the downstroke of the spike in the detailed ion-channel-based model is akin to a downhill ramp toward its resting value instead of a hard reset as assumed in the quadratic model. In fact, our observations of the estimates suggest that the penultimate term in (12) is appropriated by the estimator to match data from the upstroke of the spike whereas its intended purpose in the quadratic model is to capture the downstroke, or resetting. Furthermore, the final term in (12) is appropriated by the estimator to match data from the downstroke of the spike while its intended purpose in the quadratic model is to capture adaptation effects in the neuron. These observations suggest the need to do one of the following: (1) to pre-process the output of the detailed model to replace the ramp-like downstroke with a hard reset - this is acceptable because we are interested merely in replicating firing patterns and not subthreshold oscillation, or shapes, of action potential, however, this requires *a priori* knowledge of the reset voltage; and (2) to replace the hard reset term in (12) with a ramp-like term, however, this would require an adjustment in the quadratic model to suspend the original system dynamics during that interval. Moreover, in addition to utilization of weights to enforce good estimation of the behavior around the spike instants, hard bounds could be enforced on estimates for parameters whose signs are known *a priori* in order to ensure better prediction, e.g., the parameter encoding for reset after a spike should be upperbounded by zero. In general, we remark that system identification theory states that the best approximate (i.e., reduced-order) description of a system depends on the particular type of input used [15]. Specific to the adaptive quadratic model of [11], we remark that it can qualitatively reproduce a slew of neuronal firing patterns, however, as stated in [14], the model cannot quantitatively represent the upstroke of a spike unless a voltage-dependence of parameters is assumed.

We note that the exact spike time is highly sensitive to parameter estimation error, i.e., the results suggest that even small percentage errors in parameter estimation might cause the spike location of the prediction and the reference to be mismatched, however, the firing rate and patterns are not very sensitive to parameter estimation. It is actually more important to replicate the rate of firing and the pattern since mean firing rate carries information about experimental conditions, furthermore, a specific firing pattern may convey significant behavioral information [25] and, for large networks of spiking neurons, the firing rate of each neuron in the network is a function of the firing rates of all other neurons [26]. In any case, due to inherent noise in experimental environments, perfect estimation is nearly impossible. Furthermore, it is more practical to determine a parameter distribution, since experimental data under different conditions suggest that there is a stochastic variable in neuronal activity [27].

V. Conclusion

In this brief, a weighted least squares approach to estimate parameters in a quadratic spiking neuron model has been proposed. Several tests were run to demonstrate the robustness of this approach to noise. Results on detailed simulation and *in-vitro* experimental data suggested directions for improvement. Compared with existing methods, the proposed method is systematic and computationally inexpensive, this was expected to significantly speed up characterization for biologically relevant neuronal models. Future work will focus on model modification so it can explain detailed simulation/experimental data under different input types.

References

[1] A. Hodgkin and A. Huxley, "A quantitative description of membrane current and its application to conduction and excitation in nerve," *J. Physiol.*, vol. 117, no. 4, pp. 500–544, Aug. 1952.

[2] W. Gerstner and W. M. Kistler, *Spiking Neuron Models: Single Neurons, Populations, Plasticity*. Cambridge, U.K.: Cambridge Univ. Press, 2002.

[3] J. Vreeken, "Spiking neural networks: An introduction," *Artif. Intel. Lab., Intel. Syst. Group*, vol. 8, no. 3, pp. 1–5, 2003.

[4] W. Maass, "Networks of spiking neurons: The third generation of neural network models," *Neural Netw.*, vol. 10, no. 9, pp. 1659–1671, 1997.

[5] D. Goodman and R. Brette, "Brian: A simulator for spiking neural networks in python," *Front. Neuroinf.*, vol. 2, no. 5, pp. 1–12, 2008.

[6] D. B. Thomas and W. Luk, "FPGA accelerated simulation of biologically plausible spiking neural networks," in *Proc. IEEE Symp. Field Program. Custom Comput. Mach.*, Napa, CA, Apr. 2009, pp. 45–52.

[7] R. Brette, M. Rudolph, T. Carnevale, M. Hines, D. Beeman, J. M. Bower, M. Diesmann, A. Morrison, P. H. Goodman, and F. C. Harris, "Simulation of networks of spiking neurons: A review of tools and strategies," *J. Comput. Neurosci.*, vol. 23, no. 3, pp. 349–398, 2007.

[8] J. Schemmel, A. Gruebl, K. Meier, and E. Mueller, "Implementing synaptic plasticity in a VLSI spiking neural network model," in *Proc. Int. Joint Neural Netw. Conf.*, 2006, pp. 1–6.

[9] Y. Meng, Y. Jin, and J. Ying, "Modeling activity-dependent plasticity in bcm spiking neural networks with application to human behavior recognition," *IEEE Trans. Neural Netw.*, vol. 22, no. 12, pp. 1952–1966, Dec. 2011.

[10] N. R. Luque, J. A. Garrido, R. R. Carrillo, O. J.-M. D. Coenen, and E. Ros, "Cerebellar input configuration toward object model abstraction in manipulation tasks," *IEEE Trans. Neural Netw.*, vol. 22, no. 8, pp. 1321–1328, Aug. 2011.

[11] E. M. Izhikevich, "Simple model of spiking neurons," *IEEE Trans. Neural Netw.*, vol. 14, no. 6, pp. 1569–1572, Nov. 2003.

[12] A. N. Burkitt, "A review of the integrate-and-fire neuron model: I. Homogeneous synaptic input," *Biol. Cybern.*, vol. 95, no. 1, pp. 1–19, Apr. 2006.

[13] E. M. Izhikevich, "Which model to use for cortical spiking neurons?" *IEEE Trans. Neural Netw.*, vol. 15, no. 5, pp. 1063–1070, Sep. 2004.

[14] E. M. Izhikevich, *Dynamical Systems in Neuroscience: The Geometry of Excitability and Bursting*. Cambridge, MA: MIT Press, 2007.

[15] L. Ljung, *System Identification-Theory for the User*, 2nd ed. Englewood Cliffs, NJ: Prentice-Hall, 1999.

[16] D. Haufler, F. Morin, J. C. Lacaille, and F. K. Skinner, "Parameter estimation in single-compartment neuron models using a synchronization-based method," *Neurocomputing*, vol. 70, nos. 10–12, pp. 1606–1610, Jun. 2007.

[17] R. Brette and W. Gerstner, "Adaptive exponential integrate-and-fire model as an effective description of neuronal activity," *J. Neurophysiol.*, vol. 94, no. 5, pp. 3637–3642, Jul. 2005.

[18] G. Lemasson and R. Maex, *Introduction to Equation Solving and Parameter Fitting. In: Computational Neuroscience: Realistic modeling for Experimentalists*, London, U.K.: CRC Press, 2001.

[19] A. Prinz, C. Billimoria, and E. Marder, "Alternative to hand-tuning conductance-based models: Construction and analysis of database of model neurons," *J. Neurophysiol.*, vol. 90, no. 6, pp. 3998–4015, Aug. 2003.

[20] M. C. Vanier and J. M. Bower, "A comparative survey of automated parameter-search methods for compartmental neural models," *J. Comput. Neurosci.*, vol. 7, no. 2, pp. 149–171, 1999.

[21] J. J. Slotine and W. Li, *Applied Nonlinear Control*. Englewood Cliffs, NJ: Prentice-Hall, 1991.

[22] C. Gray and D. Mccormick, "Chattering cells superficial pyramidal neurons contributing to the generation of synchronous oscillations in the visual cortex," *Science*, vol. 274, no. 5284, pp. 109–113, Oct. 1996.

[23] D. A. McCormick, Z. Wang, and J. Huguenard, "Neurotransmitter control of neocortical neuronal activity and excitability," *Cereb. Cortex*, vol. 3, no. 5, pp. 387–398, 1993.

[24] A. Destexhe, D. Contreras, and M. Steriade, "Mechanisms underlying the synchronizing action of corticothalamic feedback through inhibition of thalamic relay cells," *J. Neurophysiol.*, vol. 79, no. 2, pp. 999–1016, Feb. 1998.

[25] H. Nakahara and S. Amari, "Information-geometric measure for neural spikes," *Neural Comput.*, vol. 14, no. 10, pp. 2269–2316, 2002.

[26] N. Brunel and P. E. Latham, "Firing rate of the noisy quadratic integrate-and-fire neuron," *Neural Comput.*, vol. 15, no. 10, pp. 2281–2306, 2003.

[27] P. Lansky, P. Sanda, and J. He, "The parameters of the stochastic leaky integrate-and-fire neuronal model," *J. Comput. Neurosci.*, vol. 21, no. 2, pp. 211–223, 2006.

Complete Synchronization of Boolean Networks

Rui Li and Tianguang Chu

***Abstract*— We examine complete synchronization of two deterministic Boolean networks (BNs) coupled unidirectionally in the drive–response configuration. A necessary and sufficient criterion is presented in terms of algebraic representations of BNs. As a consequence, we show that complete synchronization can occur only between two conditionally identical BNs when the transition matrix of the drive network is nonsingular. Two examples are worked out to illustrate the obtained results.**

***Index Terms*— Boolean networks, complete synchronization, nonsingularity.**

I. Introduction

Boolean networks (BNs) have been used extensively as abstract modeling schemes for complex systems such as gene or protein webs, neural networks, and biological evolution models [1]–[5]. In a BN, the state of each node is described by a binary variable, where a value of 1 (resp., 0) means that the node is ON (resp., OFF), and every node updates its state according to a logical relationship, given in the form of a Boolean function, with other nodes in the network. Although BNs are rather simple models of real systems, they can provide a general description of the behavior at system level in most cases [6], [7]. It is therefore of interest to investigate BNs

Manuscript received October 17, 2011; revised January 9, 2012; accepted February 26, 2012. Date of publication March 14, 2012; date of current version May 2, 2012. This work was supported in part by the National Basic Research Program of China, under Grant 2012CB821200 and the National Natural Science Foundation of China, under Grant 60974064 and Grant 60736022.

The authors are with the State Key Laboratory for Turbulence and Complex Systems, College of Engineering, Peking University, Beijing 100871, China (e-mail: rui.li@pku.edu.cn; chutg@pku.edu.cn).

Color versions of one or more of the figures in this paper are available online at http://ieeexplore.ieee.org.

Digital Object Identifier 10.1109/TNNLS.2012.2190094